

## Electron-Microscope Observation of the Smectic-Nematic Transition in a Lyotropic Liquid Crystal

M. J. Sammon and J. A. N. Zasadzinski  
*AT&T Bell Laboratories, Murray Hill, New Jersey 07974*

and

M. R. Kuzma  
*Physics Department, Temple University, Philadelphia, Pennsylvania 19122*  
(Received 30 May 1986)

We observe via freeze-fracture transmission electron microscopy the transition from the disklike micellar nematic phase to the lamellar smectic phase of decylammonium chloride-ammonium chloride-water as a function of temperature. We show direct visual evidence of the size and shape of the aggregates in the nematic phase, the mechanism of the nematic-smectic transition, and the origin of the residual in-plane order in the smectic phase. These observations are consistent with previous scattering, conductivity, and NMR measurements on this system.

PACS numbers: 64.70.Md, 61.16.Di, 61.30.Eb, 64.80.Gd

Since the first observation of lyotropic nematics by Lawson and Flautt,<sup>1</sup> considerable effort has been devoted to understanding the physics and chemistry of micellar nematic and smectic phases.<sup>2-4</sup> The observable features of nematic lyotropics [dielectric ( $\epsilon_a$ ) and diamagnetic ( $\chi_a$ ) anisotropies, NMR splitting, neutron and x-ray scattering, etc.] are interpreted by the assumption that the surfactant molecules aggregate into micelles with a specific equilibrium statistical shape and symmetry. Arguments based on x-ray and neutron scattering data<sup>5-7</sup> support a disklike micellar structure of the nematic  $N_L$  phase (also known as type-II mesophases<sup>3</sup>). However, absolute dimensions cannot be directly determined by scattering techniques as the density of aggregates in the nematic phase dictates that both intramicelle and intermicelle scattering are important. Estimates of the disk diameter in  $N_L$  phases range from 6 to 100 nm.<sup>5-7</sup> Structural information about the nematic-smectic transition is nonexistent. In systems with a continuous nematic-smectic transition, including the one studied in this Letter, x-ray scattering suggests that a residual in-plane order persists into the lamellar phase, although the origin of this ordering is still speculative.<sup>7</sup>

The best method of resolving structural questions in concentrated dispersions is by freeze-fracture transmission electron microscopy. Specifically, we examined the nematic and smectic phases of the mixture decylammonium chloride (DACl)-ammonium chloride ( $\text{NH}_4\text{Cl}$ )-water (43.97:1.76:54.27 wt. %), which has the following transition temperatures:

$$T_{AN} = 32.8^\circ\text{C} \pm 0.1^\circ\text{C}, \quad T_{NI} = 47.7^\circ\text{C} \pm 0.1^\circ\text{C}.$$

The transition from smectic to nematic ( $T_{AN}$ ) in this system has been well studied in the literature and is continuous, or nearly so.<sup>7,8</sup> We present here the first direct

evidence of the shape and size of the aggregates in the  $N_L$  phase, the mechanism of the nematic-smectic transition, and the origin of the residual in-plane order in the lamellar phase.

The method used in obtaining the micrographs presented in this Letter is the jet-freeze, double-replica technique.<sup>9,10</sup> A small droplet of sample (approximately 0.1–0.5  $\mu\text{l}$ ) was trapped between two thin copper freeze-fracture planchettes [Balzers (Hudson, New Hampshire)] to form a 10–50- $\mu\text{m}$ -thick layer. During this process, a small amount of water was lost by evaporation.<sup>8</sup> The sample sandwiches were rapidly frozen ( $> 15000^\circ\text{C}/\text{sec}$ ) in the opposed, high-velocity jets of liquid propane at  $-180^\circ\text{C}$  in a Balzers Cryojet 020 apparatus. The frozen sample sandwiches were transferred to a fracture table and loaded into the vacuum chamber of a Balzers 400 freeze-etch device. At  $-170^\circ\text{C}$  and  $10^{-8}$  Torr, the fracture table was opened to separate the copper platelets and fracture the samples. A second set of samples was fractured at  $-105^\circ\text{C}$  and the same pressure (at this temperature, the vapor pressure of ice is substantially greater than the background pressure) and the fracture surface was exposed to the vacuum for 15 sec to allow a small amount of water to sublimate. Both sets of fracture surfaces appeared similar, eliminating the possibility of condensation artifacts from the residual gases in the chamber. The fracture surfaces were replicated by evaporation of a 15- $\text{\AA}$  platinum layer at a  $45^\circ$  angle, followed by about 150  $\text{\AA}$  of carbon at normal incidence for support.

In any freeze-fracture experiment, a major concern is preventing any structural rearrangement caused by freezing. With the jet-freeze technique outlined above, water is vitrified; no evidence of ice crystallization is observed.<sup>10</sup> Freeze-fracture images of the nematic phase of tobacco mosaic virus dispersions in water show that our

freezing technique preserves the orientation and distribution of rigid virus particles. The nematic order parameter measured by x-ray diffusion before freezing was identical to that measured from the micrographs.<sup>10</sup> Of course, micelles are not rigid particles; they are in exchange equilibrium with molecules in solution. An estimate of the exchange rate of a single surfactant molecule between monomer and micelle is<sup>11</sup>

$$\tau_{\text{ex}} = \nu_0^{-1} (55 \text{ mol/l}) / C_{MC},$$

where  $\nu_0$  is a typical rotation frequency for a surfactant molecule ( $\approx 10^8 \text{ sec}^{-1}$ ) and  $C_{MC}$  is the critical micelle concentration ( $10^{-4} \text{ mol/l}$  for DACl in water with  $0.6M \text{ NH}_4\text{Cl}$ <sup>12</sup>). For our system,  $\tau_{\text{ex}} > 10^{-2} \text{ sec}$ . An estimate of the rearrangement time for a micelle is  $\approx M_{\text{ag}} \tau_{\text{ex}}$ , where  $M_{\text{ag}}$  is the aggregation number. This value is greater than the time it takes to freeze a sample,  $< 10^{-2} \text{ sec}$ . We are confident that artifacts of freezing are not responsible for the structures in the micrographs.

Figure 1 is a freeze-fracture image of the  $N_L$  phase of

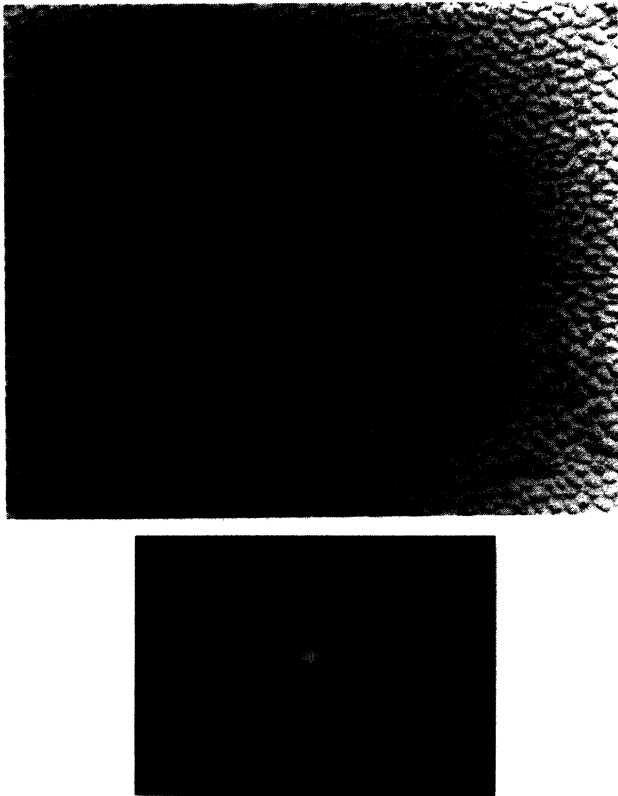


FIG. 1. The DACl system quenched from  $41^\circ\text{C}$  showing the disk-shaped micelles. The director is normal to the page. Optical transform of the negative shows a narrow distribution of intermicellar spacings of average  $105 \text{ \AA}$ . Superimposed on optical transform is a catalase crystal calibration of  $d$  spacing  $87.5$  and  $68.5 \text{ \AA}$ . Asymmetry of scattering is due to metal shadowing.

the DACl system quenched from  $41^\circ\text{C}$  along with an optical transform taken from the negative. [The bright Bragg spots on the optical transform are due to a double exposure with the optical transform of a catalase (Balzers) crystal of equal magnification used for calibration. The  $d$  spacings of catalase are  $87.5$  and  $68.5 \text{ \AA}$ .<sup>13</sup>] The aggregates appear as randomly distributed oblate ellipsoids with the nematic director roughly perpendicular to the micrograph. From the optical transform, the average center-to-center spacing of the micelles is about  $105 \text{ \AA}$  and the size distribution is narrow. The asymmetry apparent in the optical transform is caused primarily by the shadowing process, not by any asymmetry in the micelle distribution. Unidirectional metal shadowing does not provide any information on surface variations perpendicular to the shadow direction; hence the transform is zero along this direction and the scattering pattern is asymmetric.<sup>13</sup> A rough estimate of the spacing of the micelles along the director can be obtained from the shadows cast by the micelles and is about  $40 \text{ \AA}$ .

The average lateral separation of the micelles in our micrographs is larger than the  $60\text{--}65\text{-\AA}$  separations found by Holmes and Charvolin on a similar system.<sup>7</sup> There are several possible explanations of this discrepancy. The mixture examined by those authors had a ratio of  $10:1$  of  $\text{DACl}:\text{NH}_4\text{Cl}$ , while our samples were  $25:1$ . The phase diagrams of Rizzati and Gault<sup>8</sup> show that such changes in the  $\text{DACl}:\text{NH}_4\text{Cl}$  ratio make substantial changes in the transition temperatures and phase boundaries. Since the micelle size is dependent on both temperature and salt concentration, the simple fact that the nematic phase of the  $25:1$  samples occurs at a lower temperature ( $\approx 20^\circ\text{C}$  lower) than the  $10:1$  sample might explain the difference in size between our results and Ref. 7. Considering these complications, we do not believe that a serious disagreement exists between the work presented here and x-ray data.<sup>7</sup> Finally, in this system, the dimensions of the aggregates and their separations are similar; hence intra-aggregate and interaggregate interferences contribute to the x-ray scattering in the same range of scattering vectors and the two contributions cannot be directly distinguished. Therefore, assigning too much significance to the absolute dimensions obtained by treating broad, weak x-ray reflections as Bragg peaks should be avoided.<sup>7</sup>

Figure 2 shows a transition region from  $N_L$  micelles to bilayers from a sample that was quenched from  $35^\circ\text{C}$ . Part of the sample contains visually smooth lamellae (A), while other areas (B) still contain micelles that appear to have stacked into regular layers. As the micelles pack together, they align into rows and the intermicellar spacing decreases. The water separating the micelles in the plane normal to the director is most likely expelled between the layers as the transition proceeds. This is consistent with x-ray measurement of the layer spacing that show a continuous increase as the temperature is decreased.<sup>7</sup> The optical transform of this micrograph



FIG. 2. The DACI system quenched from 35°C showing the transition from nematic disklike phase to the lamellar smectic phase. Micelles stack into lamellar planes (B) and begin aligning in rows (D). Micelles at edges of growing lamellae fuse to form rodlike structures. Completed smectic layers are seen at A. Optical transform shows the increasing linear ordering and decreasing intermicellar spacing at the transition. Catalase calibration is superimposed.

clearly shows this process. The symmetric micelle scattering pattern of the nematic phase (Fig. 1) has developed a definite linear feature in Fig. 2 which extends out to smaller separations. Again, the bright spots are from a catalase calibration sample. Along the edges of layers, the micelles appear to fuse into rodlike structures (C). The directional aggregation of the micelles within the layers forms ripplelike textures (D) as they pack closer together. This observation shows the continuous nature of the nematic-smectic transition.

Figure 3 is of a sample quenched from 29°C in the lamellar phase. In the lamellar phase, the bilayers are pierced by a high density of screw dislocations, such as those that form the twist wall at the arrow.<sup>14,15</sup> A screw dislocation in a lamellar phase resembles a spiral staircase; the defect connects the aqueous (and hydrocarbon) domains of adjacent bilayers providing a continuous pathway for conduction through the layers. The density of screw dislocations increases dramatically near the lamellar-to-isotropic transition in similar systems,<sup>14</sup> and might be responsible for the anomalously high conduction normal to the bilayers observed in these phases.<sup>16,17</sup> An optical transform of the apparently smooth region at A shows the existence of a Bragg-type reflection indicating a rippling in the bilayer plane at a spacing of about 70 Å. These ripples are difficult to see in the micrographs because the surface contours that produce the variations in platinum thickness (and the optical-density modulations on the negative) are of small amplitude. Alternatively, the order within the bilayers might not be well established at this temperature. In either case, these ripples are likely the source of the diffuse, in-plane



FIG. 3. Twist wall (arrow) is smectic phase quenched from 29°C. Optical diffraction from bilayer at A shows a Bragg-type reflection at 70 Å indicative of rippled structure within bilayer planes.

scattering observed in these phases.<sup>7</sup>

In samples quenched from 27°C (Fig. 4), the ripple pattern is much more distinct. The ripples are straight and uniformly spaced over distances of about a micrometer, although the ripple directions do not appear to be correlated between layers or over longer distances within the same layer. Polarized-light microscopy indicates that the lamellar phase is optically uniaxial. Optical transforms from A and B show multiple reflections indicative of a well defined spacing of 75 Å. Surprisingly, there are also bright spots located almost perpendicular

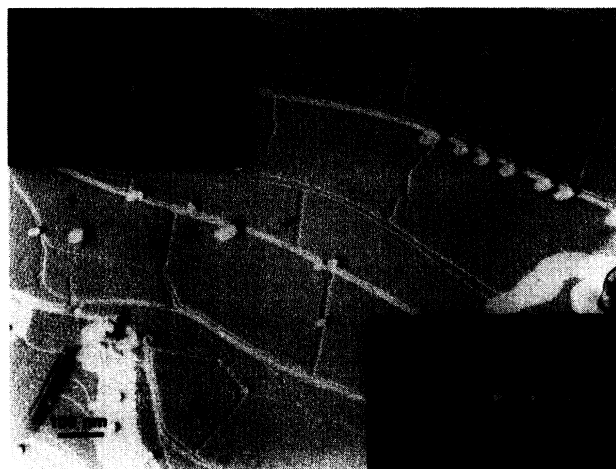


FIG. 4. Rippled texture in smectic phase quenched from 27°C and optical transforms from A and B. Multiple reflections show well defined ripple spacing of 75 Å and a modulation along the ripple of wavelength 180 Å. Micelles appear to have compacted but retain identity well into lamellar phase (arrows). Ripples change direction over short distances (C).

to the ripple reflections. The absence of first-order spots corresponding to these in-ripple reflections show that this periodicity is not a density wave, but a modulation along the ripple. Because the ripple directions change frequently within the sample (C), the ripples would appear as a diffuse ring in an x-ray experiment. The width of the ripples is close to that of the micelles in the nematic phase. The source of the modulations is likely the regular scalloped edges visible at the edges of layer steps (arrows). It appears that the micelles retain their individual identity well into the lamellar phase although some distortion of their shape occurs as they pack into well-defined rows within the bilayers. X-ray scattering shows some residual in-plane order as much as 15°C below the smectic-nematic transition.<sup>7</sup>

From our observations, we conclude the following: (1) Within the  $N_L$  phase, the micelles are independent disk-like aggregates of narrow size distribution. The degree of interconnectivity is small. (2) Near the  $N_L$ -lamellar transition, the micelles stack into layers, the water in the plane of the micelles is expelled, and the micelles pack together in equally spaced rows. (3) In the lamellar phase, distinct densely packed rows of micellar structures exist within the lamellar planes. Screw dislocations are numerous. (4) The fact that we observe distinct micelles persisting well into the smectic phase explains the small change in resistivity parallel to the director at the transition. The high density of screw dislocations that connect the aqueous domains of adjacent bilayers also contributes to the conductivity along the director.

---

<sup>1</sup>K. D. Lawson and T. J. Flautt, *J. Am. Chem. Soc.* **89**, 5489 (1967).

<sup>2</sup>A. Saupe, *Nuovo Cimento* **3**, 16 (1984).

<sup>3</sup>B. J. Forrest and L. W. Reeves, *Chem. Rev.* **81**, 1 (1981).

<sup>4</sup>J. Charvolin, *J. Chim. Phys.* **80**, 15 (1983).

<sup>5</sup>Y. Hendrix, J. Charvolin, M. Rawiso, L. Liebert, and M. C. Holmes, *J. Phys. Chem.* **87**, 3991 (1983); L. Q. Amaral, C. A. Pimental, M. R. Tavares, and J. A. Vanin, *J. Chem. Phys.* **71**, 2940 (1979).

<sup>6</sup>Y. Galerne, A. M. Figueiredo Neto, and L. Liebert, *Phys. Rev. A* **31**, 4047 (1985).

<sup>7</sup>M. C. Holmes and J. Charvolin, *J. Phys. Chem.* **88**, 810 (1984); M. Kuzma and A. Saupe, *Mol. Cryst. Liq. Cryst.* **90**, 349 (1983); P. J. Photinos, L. J. Yu, and A. Saupe, *Mol. Cryst. Liq. Cryst.* **67**, 277 (1981).

<sup>8</sup>A small water loss increases the transition temperatures without changing the nature of the transition as shown in the phase diagrams of M. R. Rizzatti and J. D. Gault, *J. Colloid Interface Sci.* **110**, 258 (1986).

<sup>9</sup>M. Mueller, N. Meister, and H. Moor, *Mikroskopie* **36**, 129 (1980).

<sup>10</sup>J. A. N. Zasadzinski and R. B. Meyer, *Phys. Rev. Lett.* **56**, 636 (1986).

<sup>11</sup>J. N. Israelachvili, S. Marcelja, and R. G. Horn, *Q. Rev. Biophys.* **13**, 121 (1980); M. R. Kuzma, *J. Phys. Chem.* **89**, 4214 (1985).

<sup>12</sup>C. Tanford, *The Hydrophobic Effect* (Wiley, New York, 1980), p. 80.

<sup>13</sup>D. L. Misell, in *Image Analysis, Enhancement and Interpretation*, edited by A. M. Glauert (North-Holland, Amsterdam, 1978), pp. 155–160, 66–75; P. R. Smith and J. Kistler, *J. Ultrastruct. Res.* **61**, 124 (1977).

<sup>14</sup>M. Kleman, C. E. Williams, M. J. Costello, and T. Gulik-Krzywicki, *Philos. Mag.* **35**, 33 (1977).

<sup>15</sup>M. Allain, *J. Phys. (Paris)* **46**, 225 (1985), and to be published.

<sup>16</sup>P. J. Photinos and A. Saupe, *J. Chem. Phys.* **84**, 517 (1986).

<sup>17</sup>N. Boden, S. A. Corne, and K. W. Jolley, *Chem. Phys. Lett.* **105**, 99 (1984).

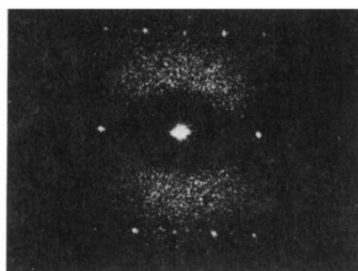
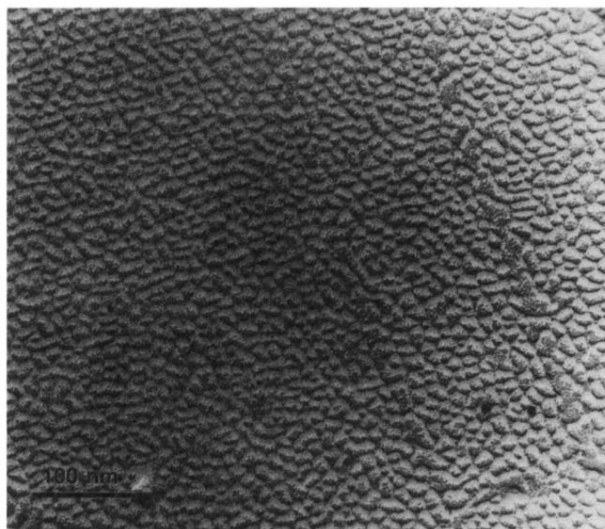


FIG. 1. The DACI system quenched from 41°C showing the disk-shaped micelles. The director is normal to the page. Optical transform of the negative shows a narrow distribution of intermicellar spacings of average 105 Å. Superimposed on optical transform is a catalase crystal calibration of  $d$  spacing 87.5 and 68.5 Å. Asymmetry of scattering is due to metal shadowing.

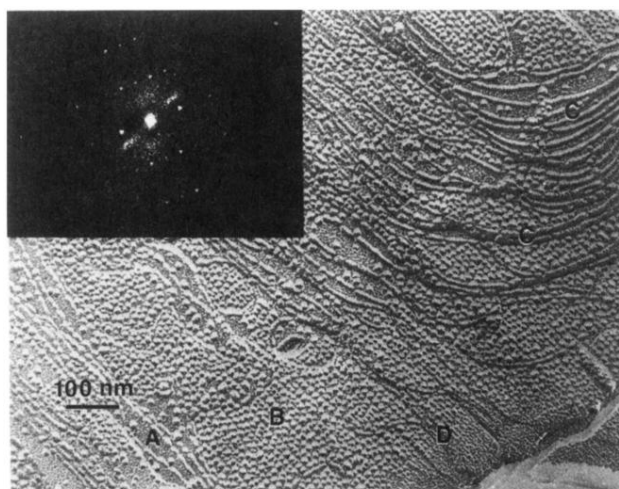


FIG. 2. The DACI system quenched from 35°C showing the transition from nematic disklike phase to the lamellar smectic phase. Micelles stack into lamellar planes (B) and begin aligning in rows (D). Micelles at edges of growing lamellae fuse to form rodlike structures. Completed smectic layers are seen at A. Optical transform shows the increasing linear ordering and decreasing intermicellar spacing at the transition. Catalase calibration is superimposed.

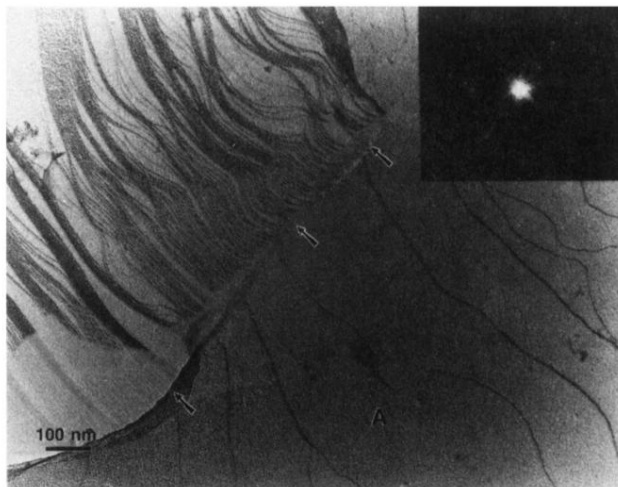


FIG. 3. Twist wall (arrow) is smectic phase quenched from 29°C. Optical diffraction from bilayer at A shows a Bragg-type reflection at 70 Å indicative of rippled structure within bilayer planes.

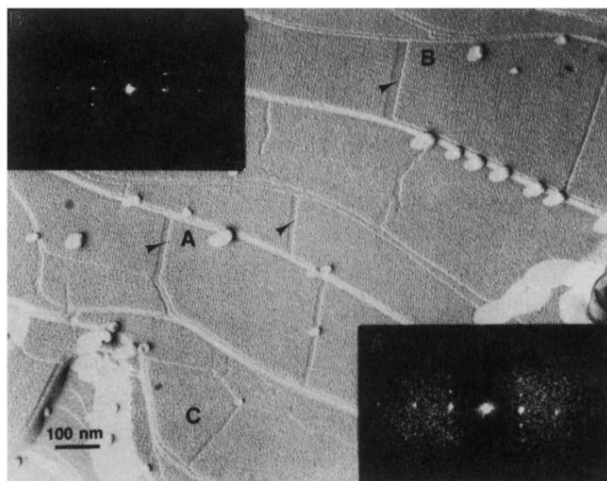


FIG. 4. Rippled texture in smectic phase quenched from  $27^{\circ}\text{C}$  and optical transforms from A and B. Multiple reflections show well defined ripple spacing of  $75 \text{ \AA}$  and a modulation along the ripple of wavelength  $180 \text{ \AA}$ . Micelles appear to have compacted but retain identity well into lamellar phase (arrows). Ripples change direction over short distances (C).